

# Self-tuning of threshold for a two-state system

Boyoung Seo<sup>1</sup>, Raishma Krishnan<sup>2</sup>, and Toyonori Munakata<sup>1\*</sup>

<sup>1</sup>*Department of Applied Mathematics and Physics,*

*Graduate School of Informatics, Kyoto University, Kyoto 606-8501, Japan*

<sup>2</sup>*Institute of Physics, Sachivalaya Marg,*

*Bhubaneswar 751005, Orissa, India*

## Abstract

A two-state system (TSS) under time-periodic perturbations (to be regarded as input signals) is studied in connection with self-tuning (ST) of threshold and stochastic resonance (SR). By ST, we observe the improvement of signal-to-noise ratio (SNR) in a weak noise region. Analytic approach to a tuning equation reveals that SNR improvement is possible also for a large noise region and this is demonstrated by Monte Carlo simulations of hopping processes in a TSS. ST and SR are discussed from a little more physical point of energy transfer (dissipation) rate, which behaves in a similar way as SNR. Finally ST is considered briefly for a double-well potential system (DWPS), which is closely related to the TSS.

PACS numbers: 05.10.Gg, 02.70.Uu, 05.40.-a

---

\*Electronic address: munakata@amp.i.kyoto-u.ac.jp

## I. INTRODUCTION

Recently constructive or beneficial roles of noise gather considerable interest in many fields, such as physical [1], and biological [2] sciences as well as engineering [3]. One of the conspicuous effects of noise or random disturbance is that it can drive a dynamical system out of an equilibrium state, thus giving a life time or Kramers time [4] to (metastable) equilibrium states.

Simulated annealing method[3], which is used to search for solutions to minimization (or more generally optimization) problems in a complex system, employs noise to prevent a search process from being trapped in local minimum(metastable) states. Sophisticated algorithms are developed to efficiently escape from local metastable states, which are useful for both simulated annealing and efficient Monte Carlo simulations.[5]

Stochastic resonance(SR)[1], which stands for a phenomenon in which information transfer from input to output signals can be significantly increased by noise with appropriate (non-zero) intensity. One can comprehend SR by considering a simple threshold system,[6] which gives 1(0) as an output signal  $x$  if input signal  $s$  plus noise  $\xi$  is larger(smaller) than a certain threshold value  $a$ . If an input signal  $s$  is always smaller than  $a$  and there is no noise,  $x$  is always equal to 0 and information transfer through the threshold system is impossible. By adding noise  $\xi$  to  $s$ , there is some possibility of  $s + \xi > a$ , producing  $x = 1$  and information about  $s$  is conveyed through the threshold system. However large noise deforms original input signals too much, leading to no correlation between  $s$  and  $x$ , resulting in no information transfer from input to output signals.

As a system similar to the threshold system mentioned above, let us consider an overdamped Brownian particle in a double-well potential driven by a sinusoidal time-periodic force, which was proposed and studied as a model for Earth's ice ages[7]. This model has an activation energy and the Gaussian Brownian noise  $\xi_G$ , which may be regarded as the threshold value  $a$  and the noise  $\xi$ , respectively in the threshold system. In this case information on input signal, such as the frequency  $2\pi\omega_0$  of the sinusoidal force, is transferred as the peak position in the power spectrum of output signal. When the variance (or temperature from the fluctuation-dissipation theorem) of  $\xi_G$  is tuned to an appropriate value, which turns out to be non-zero, the signal-to-noise ratio(SNR) attains its maximum value.

From this we may consider that SR has a close relation with synchronization, especially

when external disturbance is characterized by a frequency  $f_0 = 2\pi\omega_0$ . In this regard we mention stochastic synchronization, in which an excitable system like neurons, responds in synchrony with external disturbance(signal), which also gathers lots of interest in connection with electroreceptors in the paddlefish[8].

When input signals are subthreshold, ability of a threshold system to transfer information is considerably limited for weak noise, as mentioned above. To improve information transfer in this region, we proposed recently a simple adaptation process[9] for a threshold value  $a$  hinted by a self-tuning mechanism proposed to explain auditory sensitivity[10] when input signal becomes very weak.

In this paper we consider effects of self-tuning(ST) of the threshold value for a two-state system(TSS) driven by a sinusoidal signal. One merit of TSS is that one can calculate SNR accurately[11] by solving a differential equation, without doing numerical experiments to obtain the power spectrum, based on which SNR is usually calculated. In Sec. II we introduce our system, TSS and a closely related double-well potential system(DWPS) and propose a mechanism to control a threshold value, i.e., an activation energy. In Sec. III numerical results for SNR, the probability density for residence time[12], stochastic dynamics of threshold values and the firing rate for the TSS are presented. We show that large SNR is achieved in the small noise region as expected. In Sec. IV the adaptation process, which is governed by a threshold equation with two parameters  $\alpha$  and  $\beta$ , is studied both analytically and numerically. We discuss how these parameters affect quality of information transfer, with main emphasis put on a large noise region. Final section contains some comments on energy transfer rate from input signals to a reservoir and on a double well potential system(DWPS).

## II. MODEL

In this section we first introduce the two-state system(TSS)[11] and relate it to the double-well potential system(DWPS) for convenience for later discussions on physical aspects of the model such as energy transfer to a reservoir. The system variable  $x(t)$  at time  $t$  is assumed to take only two values,  $x_+ = 1$  and  $x_- = -1$  and transition between the two states is described by the master equation

$$dp_+(t)/dt = -w_-(t)p_+(t) + w_+(t)(1 - p_+(t)), \quad (1)$$

where  $p_+(t)$  denotes the probability that  $x(t) = x_+$  with  $p_+(t) + p_-(t) = 1$ .  $w_-(t)$  is the transition probability at time  $t$  for the particle to jump to the left( $x_-$ ) site and  $w_+(t)$  is similarly defined.

The rates  $w_+(t), w_-(t)$  are expressed in an Arrhenius form as

$$\begin{aligned} w_+(t) &= \exp[(-a + A_0 \cos(\omega_0 t))/T], \\ w_-(t) &= \exp[(-a - A_0 \cos(\omega_0 t))/T], \end{aligned} \quad (2)$$

where  $T$  measures strength of noise and  $a \pm A_0 \cos(\omega_0 t)$  denotes (time dependent) activation energy for jumping.

A physical system which is closely related to the TSS is a double-well potential system(DWPS) described by the Langevin equation

$$dx/dt = -dV(x)/dx + A_0 \cos(\omega_0 t) + f(t), \quad (3)$$

where the random force  $f(t)$  satisfies the fluctuation-dissipation relation

$$\langle f(t)f(t') \rangle = 2T\delta(t - t'), \quad (4)$$

and  $V(x)$  represents the double well potential

$$V(x) = a(x - 1)^2(x + 1)^2. \quad (5)$$

When both  $A_0$  and  $T$  are smaller than  $a$  in Eq. (5), Brownian particle described by Eq. (3) may be considered to stay either at  $x_+ = 1$  or  $x_- = -1$  for time of the order of Kramers time  $\tau_{Kr} \simeq \exp(a/T)$ [4] and occasionally jumps between  $x_+$  and  $x_-$ .

When the relaxation time  $\tau_r \simeq (8a)^{-1}$  of intrawell motion is short in the sense  $\tau_r \omega_0 \ll 1$  one can introduce the adiabatic assumption to reduce the DWPS approximately to a two-state system(TSS) described by Eq. (1).

Both TSS and DWPS are extensively studied in connection with SR and are known to show SR[1], that is, SNR shows maximum at nonzero  $T$  when other parameters charactering the system, such as activation energy  $a$  and  $\omega_0, A_0$  are kept fixed. It may be noted that for the TSS[11, 12] analytic (or integral form) results for SNR and the distribution function  $p_{f,p}(\tau)$  of the first passage time for jumping to another state are available. One merit of the TSS is that even if we take effects of self-tuning(ST) into account, we can calculate SNR by solving a coupled set of differential equations Eq. (1) and Eq. (6), to be given below,

without recourse to Monte Carlo simulations, which inevitably introduce fluctuations to power spectra and consequently to SNR.

Here we introduce a mechanism for self-tuning(ST) of the activation energy  $a$  in Eq. 2, following the prescription presented in Ref. [9]. If there occurs no jumping or activation events,  $a(t)$  simply decreases, while if a jumping event occurs  $a(t)$  increases, thus controlling the jumping or firing rate by avoiding too large or too small firing rates. To express this adaptation process mathematically, we employ the following dynamics for  $a(t)$ ,

$$da(t)/dt = -\alpha a(t) + \beta[w_+(t)p_-(t) + w_-(t)p_+(t)]. \quad (6)$$

Indeed, if we tentatively put  $\beta = 0$ ,  $a(t)$  goes to zero since  $\alpha$  is chosen to be positive. If we put  $\beta$  positive, we notice that  $a(t)$  increases in proportion to the barrier crossing rate. By this mechanism we expect that the TSS adjusts  $a(t)$ , reflecting the circumstances it is put in.

For the DWPS we propose a similar adaptation dynamics for  $a(t)$  of the form

$$da(t) \equiv a(t + dt) - a(t) = -\alpha a(t)dt + \beta \int_t^{t+dt} dt \sum_i \delta(t - t_i), \quad (7)$$

where  $t_i (i = 1, 2, \dots)$  denotes the time when  $x(t) = 1$ .

### III. NUMERICAL RESULTS FOR TSS

We first explain how one can calculate SNR for the TSS with self-tuning(ST), by slightly modifying the approach in Ref.[11].

#### A. SNR with self-tuning: methodology

Let us denote the solution to Eq. (1) and Eq. (6) as

$$p_+(t) = p_+(t|x_0, a_0, t_0), \quad a(t) = a(t|x_0, a_0, t_0), \quad (8)$$

which satisfy the initial conditions  $p_+(t = t_0|x_0, a_0, t_0) = \delta(1, x_0)$  and  $a(t = t_0|x_0, a_0, t_0) = a_0$  with  $\delta(1, x)$  denoting the Kronecker  $\delta$ , i.e.,  $\delta(1, x) = 1$  if  $x = 1$  and  $\delta(1, x) = 0$  if  $x \neq 1$ . The transition probability  $p(x, a, t|x_0, a_0, t_0)$  for  $(x(t), a(t))$  to be at  $(x, a)$  starting from  $(x_0, a_0)$

is expressed as

$$\begin{aligned}
p(x, a, t \mid x_0, a_0, t_0) &= \delta(a - a(t|x_0, a_0, t_0)) \times \\
& [ p_+(t|x_0, a_0, t_0)\delta(x - 1) \\
& + (1 - p_+(t|x_0, a_0, t_0))\delta(x + 1)].
\end{aligned} \tag{9}$$

Following MacNamara and Wiesenfeld[11] let us first introduce the time correlation function  $\phi(t, \tau|x_0, a_0, t_0)$  by

$$\begin{aligned}
\phi(t, \tau \mid x_0, a_0, t_0) &= \langle x(t)x(t + \tau)|x_0, a_0, t_0 \rangle \\
&\equiv \int da' \int da \int dx \int dy xy p(x, a', t + \tau \\
& \mid y, a, t) p(y, a, t|x_0, a_0, t_0).
\end{aligned} \tag{10}$$

After performing integration of Eq. (10) over  $y$  and  $a$  we have

$$\begin{aligned}
\phi(t, \tau \mid x_0, a_0, t_0) &= \int da' \int dx x [p_+(t|x_0, a_0, t_0) \\
& p(x, a', t + \tau | 1, a(t|x_0, a_0, t_0), t) - p_-(t|x_0, a_0, t_0) \\
& p(x, a', t + \tau | -1, a(t|x_0, a_0, t_0), t)].
\end{aligned} \tag{11}$$

Now we take the limit  $t_0 \rightarrow -\infty$  to remove  $x_0, a_0$  dependence of  $p_+, p_-$  and of  $a$  on the right hand side of Eq. (11), leading to

$$\begin{aligned}
\phi(t, \tau) &= \int da' \int dx x [p_+(t)p(x, a', t + \tau | 1, a(t), t) \\
& - p_-(t)p(x, a', t + \tau | -1, a(t), t)],
\end{aligned} \tag{12}$$

where we replace  $\lim_{t_0 \rightarrow -\infty} p_+(t|x_0, a_0, t_0)$  by  $p_+(t)$  and  $\lim_{t_0 \rightarrow -\infty} a(t|x_0, a_0, t_0)$  by  $a(t)$ .  $\int da'$  can be performed trivially to have

$$\begin{aligned}
\phi(t, \tau) &= p_+(t)[2p_+(t + \tau | 1, a(t), t) - 1] \\
& - p_-(t)[2p_+(t + \tau | -1, a(t), t) - 1].
\end{aligned} \tag{13}$$

Finally to make the function  $\phi(t, \tau)$  independent of the time variable  $t$  and also to conform to experimental situations, we take time average  $(1/\tau_p) \int_0^{\tau_p} dt$  with  $\tau_p = 2\pi/\omega_0$  to obtain

$$\begin{aligned}
\phi(\tau) &= (1/\tau_p) \int_0^{\tau_p} dt \{ p_+(t)[2p_+(t + \tau | 1, a(t), t) - 1] \\
& - p_-(t)[2p_+(t + \tau | -1, a(t), t) - 1] \}.
\end{aligned} \tag{14}$$

Numerical implementation of Eq. (14) is not difficult and the result is conveniently expressed as

$$\phi(\tau) \approx \phi_{relax}(\tau) + B \cos(\omega_0 \tau), \quad (15)$$

where  $\phi_{relax}(\tau)$  is the relaxation part, which goes to zero asymptotically as  $\tau \rightarrow \infty$ , and  $B \cos(\omega_0 \tau)$  represents the periodic part of the external field. Fourier transformation of Eq. (15) has the form

$$\tilde{\phi}(\omega) = \tilde{\phi}_{relax}(\omega) + B[\delta(\omega - \omega_0) + \delta(\omega_0 + \omega)], \quad (16)$$

and SNR is define here as

$$R_{SN} = B/\tilde{\phi}_{relax}(\omega_0), \quad (17)$$

## B. Numerical results for SNR and other quantities

It is noted that we take  $\omega_0 = 0.5$  and  $A_0 = 0.3$  in the following. In Fig.1 is plotted SNR for systems with self-tuning( $\alpha = 0.03$  and  $\beta = 0.1, C \equiv \alpha/\beta = 0.3$ ) and without self-tuning( $a = 0.5$ ). We observe that SNR is improved by self-tuning in the low temperature region. This is confirmed from the first-passage time distribution function  $p_{f.p}(\tau)$  shown in Fig. 2 for the two systems marked by black circle with ST and by white circle( without ST) in Fig.1 ( $T = 0.15$ ). These  $p_{f.p}(\tau)$  are obtained by Monte Carlo simulations, in which we actually followed particle motion with the hopping rate given by Eq. (2) and obtain a histogram of the first passage time  $\tau$ . For a system with ST(Fig. 2a) we notice that most of the particles hop, taking the first chance of low activation energy. This is in contrast with the system without ST(Fig. 2b), for which we observe many bumps of probability with the spacing  $\tau_p = 2\pi/\omega_0$ . [12–14] We discuss now the overall  $T$ -dependence of SNR shown in Fig.1 based on time-averaged activation energy(Fig. 3a),  $\bar{a} = \tau_p^{-1} \int_0^{\tau_p} a(t)$  with  $\tau_p \equiv 2\pi/\omega_0$  and on a time-averaged firing rate  $\overline{fr}$  similarly defined as  $\bar{a}$ (Fig. 3b). In the low temperature region ( $T < 0.25$ ), the firing rate  $\overline{fr}$  is increased since self-tuning(ST) lowers the activation barrier  $\bar{a} (< a = 0.5)$ . However in the high temperature region( $T > 0.25$ ) where noise intensity is high, SNR is deteriorated by ST due to considerable increase of  $\bar{a}$ , which results in rapid decrease of  $\overline{fr}$  compared with the fixed threshold case(Fig.3). Firing events are in general useful for information transfer and our results suggests that rapid growth of  $\bar{a}$  as  $T$  increases

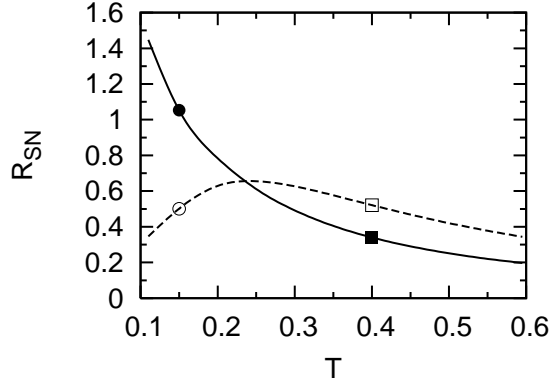


FIG. 1: SNR ( $R_{SN}$ ) as a function of noise intensity  $T$  for system with(solid curve) and without(dashed curve) ST. For ST we use  $\alpha = 0.03$  and  $\beta = 0.1$  in Eq. (6). The barrier height is set  $a = 0.5$  for the system without ST. Here and hereafter  $\omega_0$  and  $A_0$  are always set to be  $\omega_0 = 0.5$  and  $A_0 = 0.3$ .

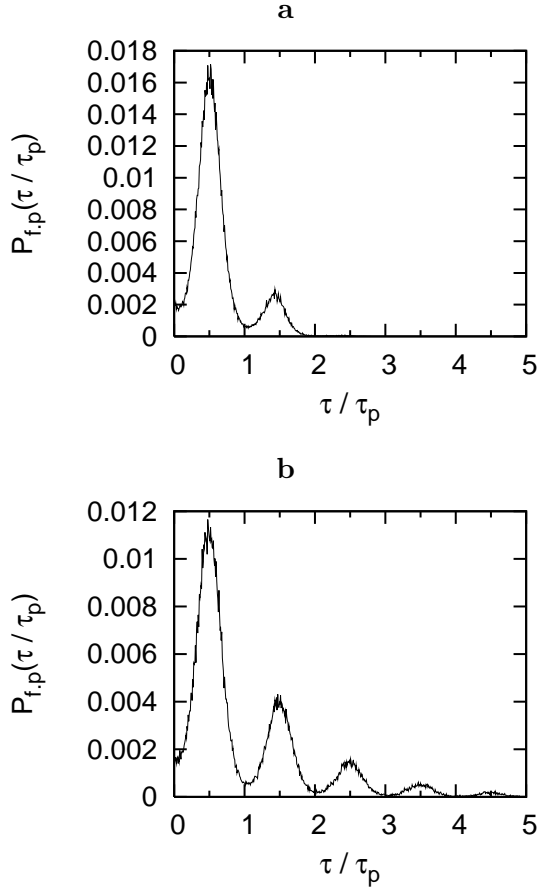


FIG. 2: First passage time distribution functions for the system marked by black circle(a) and by the white circle(b) in Fig. 1.

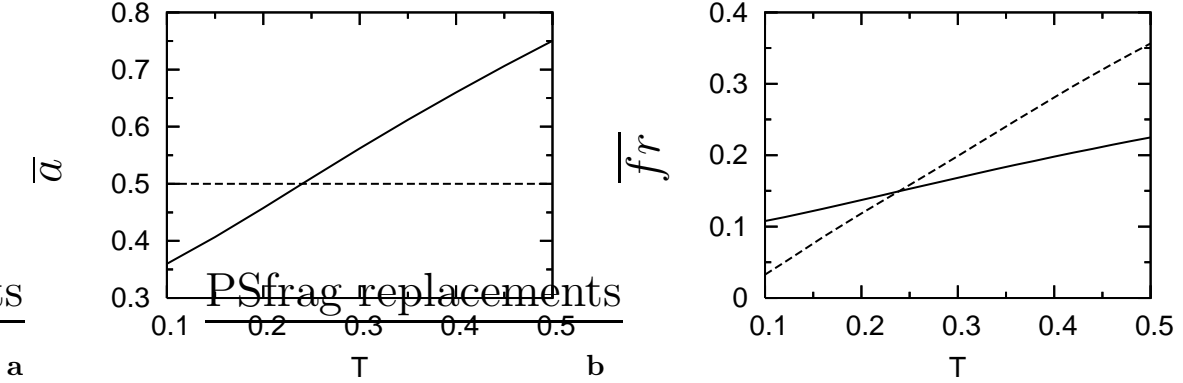


FIG. 3: Time-averaged activation energy  $\bar{a}$  (a) and time-averaged firing rate  $\overline{fr}$  as functions of  $T$ (b). Parameter values used for the solid and dashed curves correspond to the ones in Fig.1.

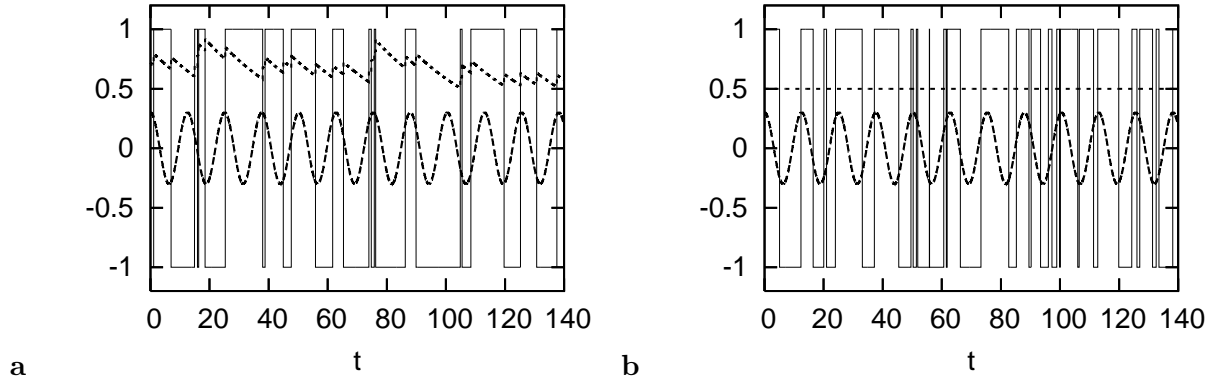


FIG. 4: Dynamical behavior  $x(t) = \pm 1$  (full curves) and  $a(t)$ (dotted curves) from Monte Carlo simulations together with the sinusoidal signals  $A_0 \cos(\omega_0 t)$ (dashed curves) for the system marked by the black squares(a) and the white squares(b) with  $\alpha = 0.03$  and  $\beta = 0.1$ .

is not welcome from the point of information processing by a threshold device. Behavior of  $\bar{a}$  and  $\overline{fr}$  depend on the parameters  $\alpha$  and  $\beta$  in Eq. (6) and this will be considered in the next section.

Before proceeding to this problem, we show a typical example of Monte Carlo trajectories  $(x(t), a(t))$  together with the input signal  $A_0 \cos(\omega_0 t)$  in Fig. 4a for the system marked by black squares(a) and white squares(b), belonging to a high  $T$  region( $T = 0.4$ ). When  $T$  and consequently noise are large, we have some chances of successive hopping events as shown in Fig. 4. In this case the activation energy  $a(t)$  increases rapidly as shown in Fig. 4a( typically around  $t \simeq 80$ ) due to ST, which inhibits a firing event on average for some time. That is, in our Monte Carlo simulations we increase  $a(t)$  by  $\beta$  whenever there occurs a

hopping event(see Eq. (6)). From this we intuitively see that large  $\beta$  values makes  $a(t)$  large, resulting in small  $fr(t)$ . With these preparations we now consider  $\alpha$  and  $\beta$  dependence of SNR.

#### IV. THRESHOLD DYNAMICS AND SNR

Now let us consider Eq. (6), which describes time evolution of the barrier height  $a(t)$ , and express it as

$$da/dt = -\alpha a(t) + \beta fr(t), \quad (18)$$

where  $fr(t)$  denotes a firing rate at time  $t$ . Since we are mainly interested in a subthreshold situation (i.e.  $a(t) > A_0$ ) and a large  $T$  region where ST did not work well compared with the weak noise region(see Fig.1), we neglect for qualitative discussion  $A_0/T$  in Eq. (2) and obtain, with a use of simple form for Kramers rate[4],

$$(\alpha/\beta)\bar{a} \equiv C\bar{a} = \exp(-\bar{a}/T), \quad (19)$$

after time averaging both sides of Eq. (18) for one period  $\tau_p = 2\pi/\omega_0$  of the external

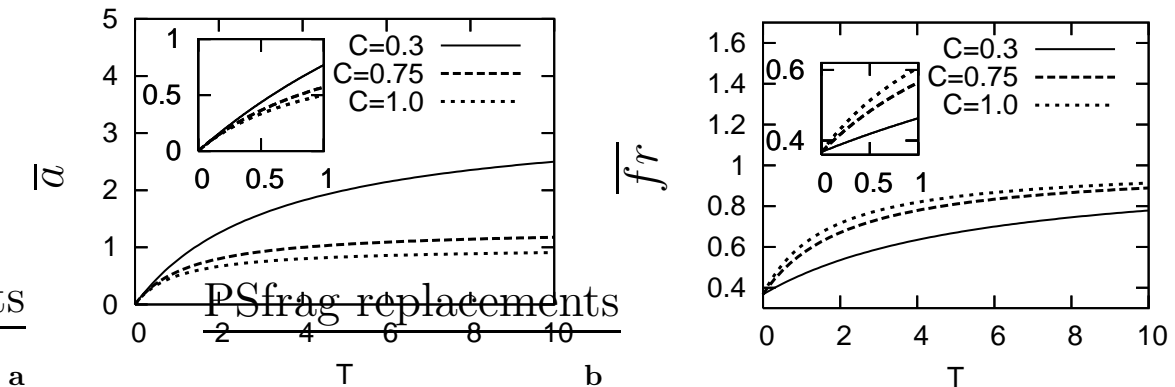


FIG. 5: Time averaged activation energy  $\bar{a}$ (a) and time-averaged firing rate  $\overline{fr}$ (b) as functions of  $T$  from Eq. (19)

field. From this we see that at large  $T$ ,  $\bar{a} \rightarrow 1/C$  and  $\overline{fr} \rightarrow (1 - 1/(TC))$ . In Fig. 5a we show  $\bar{a}$  as a function of  $T$ , which is obtained by solving Eq. (19) for three values of  $C \equiv \alpha/\beta$  ( $C = 0.3, 0.75, 1.0$  from above). We notice that the barrier height  $\bar{a}$  remains small even for large  $T$  when  $C \equiv \alpha/\beta$  becomes large. The firing rate  $\overline{fr}$ , calculated from Eq. (2)

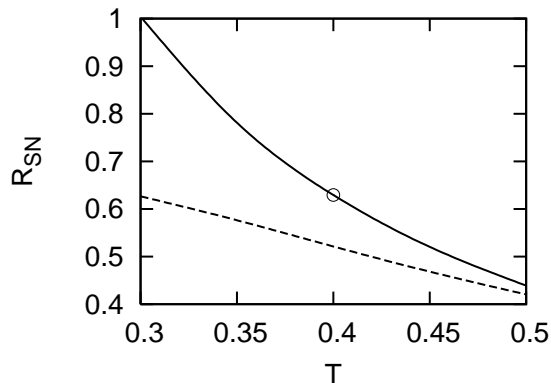


FIG. 6: SNR ( $R_{SN}$ ) with ST( $\alpha = 0.03, \beta = 0.04, C = 0.75$ ) (full curve) and without ST(dashed curve).

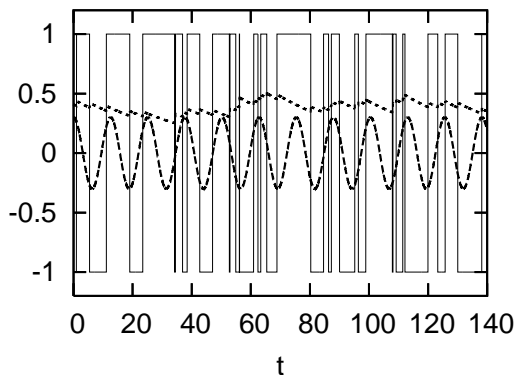


FIG. 7: Dynamical behavior  $x(t) = \pm 1$  (full curves) and  $a(t)$ (dotted curves) from Monte Carlo simulations together with the sinusoidal signals  $A_0 \cos(\omega_0 t)$ (dashed curves) for the system marked by the white circle in Fig. 6.

, Eq. (6), and Eq. (19), is shown in Fig. 5b( $C = 0.3, 0.75, 1.0$  from below). Reflecting the fact that  $\bar{a}$  does not increase rapidly with  $T$  when  $C$  is large, the firing rate seems to remain large in a large  $T$  region when  $C$  becomes slightly larger than 0.3.

Guided by this observation we choose  $C = 0.75$  ( $\alpha = 0.03$  and  $\beta = 0.04$ ) and plot SNR in Fig. 6 as a function of  $T$ . Compared with the solid curve in Fig. 1 we notice that SNR is improved considerably and our ST seems to work well even in the high  $T$  region by choosing proper values for  $C = \alpha/\beta$ .

Details of dynamics ( $x(t), a(t)$ ) are shown in Fig. 7 for the system marked with a white circle in Fig. 6. This should be compared with the dynamics in Fig. 4a which is characterized

by different parameter values( $\alpha = 0.03, \beta = 0.1, C = 0.3$ ). By choosing a smaller value for  $\beta(= 0.04)$ (keeping  $\alpha$  fixed to 0.03) we could prevent the activation energy becoming too large and this contributes to making SNR large.

## V. ENERGY TRANSFER, DWPS AND CONCLUSION

In this section we consider briefly energy transfer from input signals to the reservoir(i.e. dissipation) and the DWPS, Eqs. (3-5) before concluding this paper.

The hopping rate, Eq. (6), can be rewritten as

$$\begin{aligned} w_+(t) &= \exp[-(V_s - V_1(t))/T], \\ w_-(t) &= \exp[-(V_s - V_{-1}(t))/T], \end{aligned} \quad (20)$$

with  $V_s(= a)$  and  $V_{\pm 1}(t)$  the energy at the saddle point( $x = 0$ ) and at the position  $x = \pm 1$ , respectively. If  $x(t)$  changes at  $t = t_1$  from -1 to 1, the energy  $\Delta E(t_1)$  transferred from the signal to the reservoir is given by  $\Delta E = -(V_1(t_1) - V_{-1}(t_1)) = 2V_{-1}(t_1)$ . Dividing all the energy  $\sum_i \Delta E(t_i)$  by the experimental duration  $\tau_{exp}$  and  $\bar{a}$ , we have

$$E_{s \rightarrow r} = \sum_i \Delta E(t_i) / (\tau_{exp} \bar{a}), \quad (21)$$

which was obtained by Monte Carlo experiments.

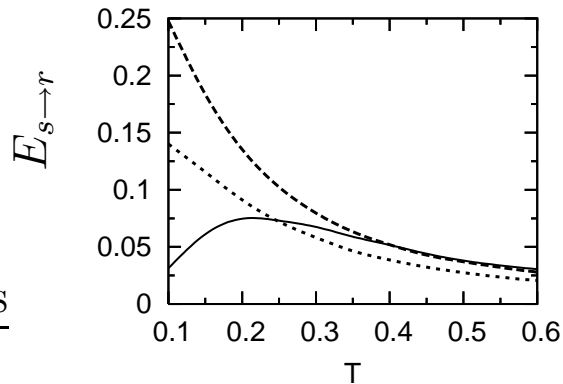


FIG. 8: Energy transfer rate  $E_{s \rightarrow r}$  as a function of  $T$  for s system without ST(full curve) and with ST with  $\alpha = 0.03, \beta = 0.1$  (dotted curve) and  $\alpha = 0.03, \beta = 0.04$  (dashed curve).

In Fig. 8 is plotted  $E_{s \rightarrow r}$  as a function of  $T$ . The dotted curve( $\alpha = 0.03, \beta = 0.04$ ), the dashed curve( $\alpha = 0.03, \beta = 0.1$ ), and the full curve correspond to the systems represented by

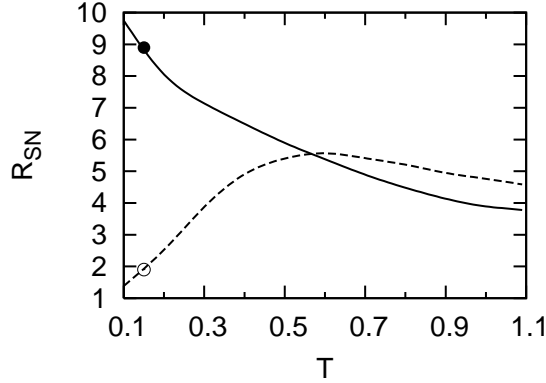


FIG. 9: SNR ( $R_{SN}$ ) for DWPS with ST(full curve) and without ST(dashed curve). For ST we use  $\alpha = 0.05$ ,  $\beta = 0.05$  in Eq. (7) and the barrier height is set  $a = 1$  for the system without ST where  $A_0 = 0.8$  and  $\omega_0 = 0.5$ .

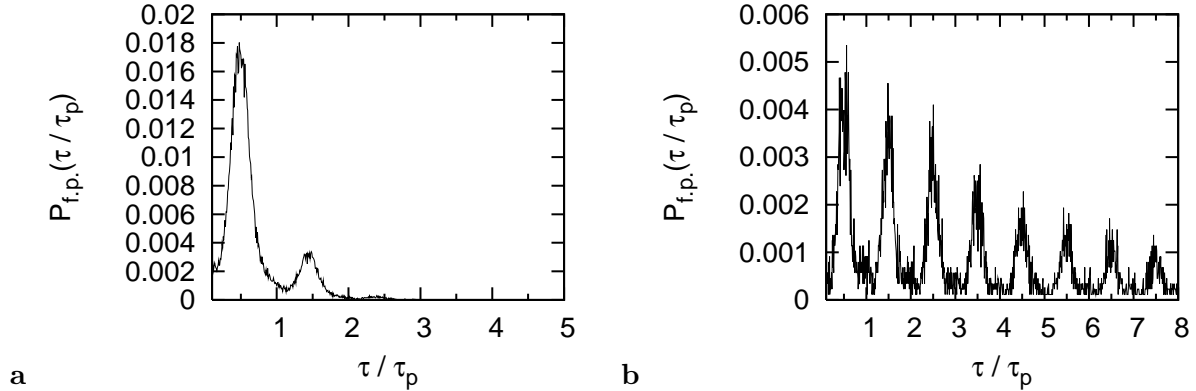


FIG. 10: First passage time distribution function  $p_{f.p.}(\tau/\tau_p)$  for DWPS with ST(a) and without ST(b) at  $T = 0.15$ . Parameter values characterizing the system is the same with those for Fig. 9.

the full curve in Fig. 6, the full curve in Fig. 1 and the dashed curve in Fig. 1, respectively. We see that SNR and  $E_{s \rightarrow r}$  show surprisingly similar behaviors. This is rather natural since both quantities depend on the firing rate and the firing timing in similar ways. Especially the firing timing is important for both SNR and  $E_{s \rightarrow r}$ . When a hopping event from  $x = -1$  to  $x = 1$  occurs at time  $t_1$ , maximum energy transfer is achieved when  $V_{-1}$  becomes maximum at time  $t_1$ . This synchrony is evidently reflected to SNR. As noted in Sec. I the synchrony is also important for SNR.

Final comment is on the double-well potential system(DWPS), Eqs. (3-5). Since TSS and DWPS describe similar hopping events under time periodic signals, we expect that

both systems share common properties, especially in relation to ST and SR. Fig. 9 shows SNR of DWPS with (full curve) and without (dashed curve) ST, where SNR is defined as the ratio  $P(\omega_0)/[P(\omega_0 - d\omega)/2 + P(\omega_0 + d\omega)/2]$  with  $P(\omega)$  denoting the power spectral density at frequency  $\omega$  and  $d\omega$  is the frequency mesh size in numerical calculations of  $P(\omega)$ . This should be compared with Fig.1 for TSS. Corresponding to Fig. 2, we compare  $p_{f,p}(\tau)$  for the two systems marked by a white and black circle in Fig. 9. in Fig.10. From these results it is seen that TSS and DWPS behave similarly with respect to response to and information transfer of the periodic signals.

In this paper we applied a ST mechanism, Eq. (6), to TSS, Eq. (1) and confirmed that better SNR is simply obtained by ST mechanism for small fluctuation (i.e. low  $T$ ) region. Tuning of the parameters  $\alpha$  and  $\beta$  was guided by a simple equation (19), leading to better SNR even for a high  $T$  region. Energy transfer or dissipation rate was also studied and this quantity (21) turned out to be able to play a similar role as a measure for information processing ability of a threshold device.

- 
- [1] V. S. Anishchenko, V. V. Astakhov, A. B. Neiman, T. E. Vadivasova, and L. Schimansky-Geier, *Nonlinear Dynamics of Chaotic and Stochastic Systems*, (Springer, Berlin, 2002). L. Gammaitoni, P. Hänggi, P. Jung, and F. Marchesoni, *Rev. Mod. Phys.* **70**, 223 (1998).
  - [2] P. Reimann, *Phys. Rep.* **361**, 57 (2002). F. Jülicher, A. Ajdari, and J. Prost, *Rev. Mod. Phys.* **69**, 1269 (1997).
  - [3] S.Kirkpatrick, C. D. Gelatt, and M. P. Vecchi, *Science* **220**, 671 (1983).
  - [4] H. A. Kramers, *Physica* **7**, 284 (1940). S. Chandrasekhar, *Rev. Mod. Phys.* **15**, 1 (1943), in *Selected Papers on Noise and Stochastic Processes*, edited by N. Wax, (Dover Publications, New York 1954).
  - [5] A. K. Hartmann, and H. Rieger, *Optimization Algorithms in Physics*, (Wiley-VCH, Berlin 2002).
  - [6] F. Marchesoni, F. Apostolico, and S. Santucci, *Phys. Rev. E* **59**, 3958 (1999). F. Apostolico, L. Gammaitoni, F. Marchesoni, and S. Santucci, *Phys. Rev. E* **55**, 36 (1997).
  - [7] R. Benzi, S. Sutera, and A. Vulpiani, *J. Phys. A* **14**, L453 (1981).
  - [8] A. B. Neiman, D. F. Russel, X. Pei, W. Wojtenek, J. Twitty, E. Simonotto, B. A. Wetting,

- E. Wagner, L. A. Wilkens, F. Moss, *Int. J. Bifurcation Chaos*, **10**, 2499 (2000).
- [9] T. Munakata, T. Hada, and M. Ueda, *Physica A*. **375**, 492 (2007).
- [10] W. Denk, W. W. Webb, A. J. Hudspeth, *Proc. Natl. Acad. Sci. USA* **86**, 5371 (1989). S. Camalet, T. Duke, F. Jülicher, J. Prost, *Proc. Natl. Acad. Sci. USA* **97**, 3183 (2000).
- [11] B. McNamara, and K. Wiesenfeld, *Phys. Rev. A*. **39**, 4854 (1989).
- [12] T. Zhou, F. Moss, and P. Jung, *Phys. Rev. A* **42**, 3161 (1990).
- [13] L. Gammaitoni, F. Marchesoni, E. Menichella-Saetta, and S. Santucci, *Phys. Rev. Lett.* **62**, 349 (1989).
- [14] L. Gammaitoni, F. Marchesoni, and S. Santucci, *Phys. Rev. Lett.* **74**, 1052 (1995).